cycle. The vacuum chamber is then vented to the atmosphere. The interelectrode spacing is then also very briefly vented to the atmosphere through a bellows-type valve. The outgassed interelectrode assembly subsequently absorbs some of the gas that is trapped in the interelectrode spacing, thereby lowering the pressure of the air trapped in the interelectrode spacing. Knowing this pressure drop and the total volume of the interelectrode assembly, one can determine the quantity of gas absorbed. Carrying out the same procedure after any desired number of discharges of the accelerator permits one to determine the additional amount of gas removed because of accelerator operation. Figure 4 shows the quantity of gas absorbed as a function of time after pump-down and after operating the accelerator for 50 and 3600 consecutive discharges. The amount of gas absorbed after accelerator operation is the difference between the pump-down curve and the curve obtained with the accelerator in operation. For the particular device tested, this amount could exceed 10^{-6} lb within a relatively short period of time. This is roughly an order of magnitude larger than the quantity of gas injected per discharge. From Fig. 4, one can see that an outgassed electrode can absorb air for as long as 80 hr. This amount usually depended on how "deeply" the assembly was outgassed and on the length of time the assembly was allowed to absorb air at atmospheric pressure.

This capping technique also permitted a check to be made on the effect of oil-vapor contamination. Using the water-break test,[1] it has been established that oil-vapor contamination exists. Since the water-break test is sensitive to a monolayer of organic contaminants, oil-vapor contamination to within a monolayer could not be ruled out. Since the impulse and its variation were substantially the same, independent of whether the interelectrode spacing was exposed to the vacuum chamber or sealed from it by the cap during pump-down, it can be deduced that oil-vapor contamination cannot account for the observed impulse dropoff. The available evidence points more strongly toward the effect of outgassing.

Erosion Studies

Since measurements have shown that large quantities of gas are rapidly absorbed by an accelerator after its removal from a vacuum environment, it was concluded that erosion studies based upon weight measurements of the accelerator components could not be considered reliable. The technique developed to determine erosion involved the use of two sets of the insulator-electrode assembly. These were weighed differentially against each other before accelerator operation. One of these sets was installed on the accelerator, whereas the other set was placed in the vacuum chamber. After accelerator operation and a cooling period in the vacuum chamber, both sets were removed and again weighed against each other. It has been observed that the new weight differential

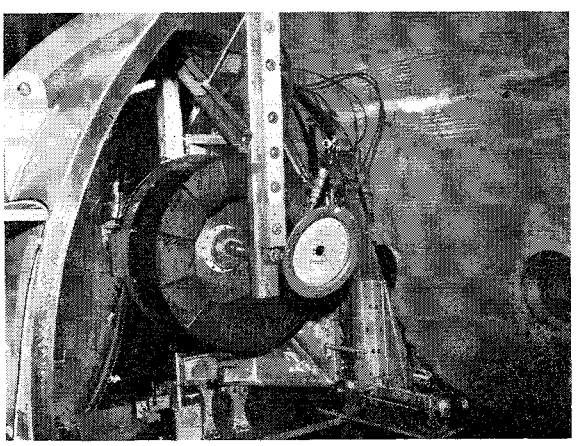

Fig. 3 Capping mechanism engaged.

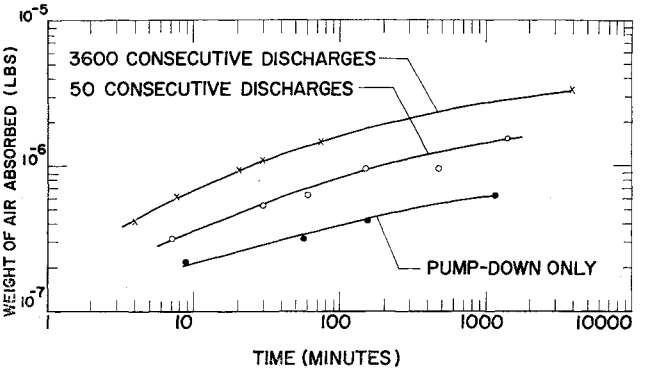

Fig. 4 Quantity of gas absorbed by electrode-insulator assembly.

remained constant within 0.0003 g for a period as long as 80 hr after removal from the vacuum chamber, even though both sets individually absorbed quantities of air several orders of magnitude larger than this constant weight difference. This constant difference in weight between the two assemblies was taken as the more reliable measure of the erosion.

A typical test carried out over 25,300 consecutive discharges provided the following data. The anode ablated the most. Its weight change was 0.022%, or the average total depth of erosion was 13.7×10^{-5} cm. The mykroy insulator was intermediate in ablation. Its weight change was 0.004%, or the average total depth of erosion was 5.65×10^{-5} cm. The inner electrode, the cathode, eroded the least. It underwent a 0.001% weight change. Its average depth of erosion was 1.13×10^{-5} cm. The average mass eroded per discharge was found to be of the order of 3.77×10^{-9} lb. This is roughly two orders of magnitude less than the total amount of neutral gas injected per discharge.

The contribution of surface effects to the discharge mechanism during prolonged periods of operation can appreciably affect the long-time performance of a pulsed plasma accelerator.

Reference

[1] Feder, D. O. and Koontz, D. E., "Detection removal and control of organic contaminants in the production of electron devices," *Symposium on Cleaning of Electronic Devices, Components and Materials*, American Society for Testing Materials Special Tech. Publ. 246, pp. 40–65 (1959).

A Flutter Design Parameter to Supplement the Regier Number

FRANK J. FRUEH*
Giannini Controls Corporation, Malvern, Pa.

Introduction

THOSE in the field of aeroelasticity realize the complexity of determining a solution for flutter and dynamic response. They have long strived for approximations and trends of the solution in terms of design parameters for use in design evaluation. One parameter that has been indicative of the trend of the flutter solution is the Regier number; this number is a nondimensionalized measure of the torsional

Received March 11, 1964. The efforts reported in this Technical Note were sponsored by the Air Force Office of Scientific Research Office of Aerospace Research under Contract AF 49(638)-1015.

* Chief, Theoretical Dynamics, Astromechanics Research Division.

stiffness required for netural stability and is defined to be $b\omega_\alpha\mu^{1/2}/a$. The Regier number has proved to be useful in the design stage of aircraft and wind-tunnel models but is limited to subsonic trends. This paper is written to present the development of a flutter design parameter that is the supersonic equivalent of Regier number and is sufficiently general to encompass the Regier number.

Technical Derivation

In order to develop a meaningful parameter for use in design evaluation of system aeroelastic integrity, it is necessary to start with the system's force equations, which describe the dynamic response of the system. From Lagrange's equation, the equations of motion in matrix form are (see Ref. 1 for further details)

$$[M_{ii}(S^2 + 2\zeta_i\omega_i S + \omega_i^2)]\{\xi_j\} = \{Q_j\} \tag{1}$$

where

M_{ii} = generalized mass of the ith mode
S = Laplace transform
ζ_i = structural viscous damping coefficient of the ith mode
ω_i = structural resonant frequency of the ith mode
ξ_j = generalized coordinate of the jth mode
Q_j = generalized applied force on the structure

For the case of an aeroelastic system, the Q_j are the aerodynamic coupling terms whose definition depends on the many assumptions associated with aerodynamic theory (for example, linearity, potential theory, speed range, etc.). However, trends are best shown by simplified analyses, and many significant dynamic characteristics have been explained in Refs. 2–4 by such analyses. These analyses assumed the validity of first-order piston theory aerodynamics; from these references, the equations of motion of a pitch-plunge uniform wing are given by

$$\begin{bmatrix} \{m(S^2 + 2\zeta_h\omega_h S + \omega_h^2) + 4\rho abS\} & \{mbx_\alpha S^2 + 4\rho ab[V + bS(1 - 2x_0)]\} \\ [mbx_\alpha S^2 + 4\rho ab(1 - 2x_0)S] & \{I_\alpha(S^2 + 2\zeta_\alpha\omega_\alpha S + \omega_\alpha^2) + 4\rho ab^2[V(1 - 2x_0) + 4bS(\tfrac{1}{3} - x_0 + x_0^2)]\} \end{bmatrix} \begin{bmatrix} h \\ \alpha \end{bmatrix} = 0 \tag{2}$$

The parameters are defined as $\mu \equiv m/4\rho b^2$, $I_\alpha \equiv mr_\alpha{}^2b^2$, $\omega_A \equiv a/\mu b$ and are incorporated into the forementioned equations to obtain

$$\begin{bmatrix} S^2 + 2\zeta_h\omega_h S + \omega_h^2 + \omega_A S & x_\alpha S^2 + (\omega_A V/b) + \omega_A S(1 - 2x_0) \\ x_\alpha S^2 + \omega_A S(1 - 2x_0) & \{r_\alpha{}^2(S^2 + 2\zeta_\alpha\omega_\alpha S + \omega_\alpha^2) + (\omega_A V/b)(1 - 2x_0) + \omega_A S(\tfrac{1}{3} - 4x_0 + 4x_0^2)\} \end{bmatrix} \begin{bmatrix} h/b \\ \alpha \end{bmatrix} = 0 \tag{3}$$

The use of these equations to study trends of system stability is very analogous to similitude analyses, in that each parameter must be matched or scaled in order to duplicate dynamic characteristics of one system by another system. It is usual to nondimensionalize the parameters of the equation, and, to do this, the terms are divided by a reference frequency squared, commonly the torsional frequency. The equations now are

$$\begin{bmatrix} \bar{S}^2 + 2\zeta_h\dfrac{\omega_h\bar{S}}{\omega_\alpha} + \dfrac{\omega_h{}^2}{\omega_\alpha{}^2} + \dfrac{\omega_A\bar{S}}{\omega_\alpha} & x_\alpha\bar{S}^2 + \dfrac{\omega_A V}{b\omega_\alpha{}^2} + \dfrac{\omega_A\bar{S}}{\omega_\alpha}(1 - 2x_0) \\ x_\alpha\bar{S}^2 + \dfrac{\omega_A}{\omega_\alpha}\bar{S}(1 - 2x_0) & r_\alpha{}^2(\bar{S}^2 + 2\zeta_\alpha\bar{S} + 1) + \dfrac{\omega_A V}{b\omega_\alpha{}^2}(1 - 2x_0) + (\tfrac{4}{3} - 4x_0 + 4x_0^2)\dfrac{\omega_A\bar{S}}{\omega_\alpha} \end{bmatrix} \begin{bmatrix} h \\ \bar{b} \\ \alpha \end{bmatrix} 0 = \tag{4}$$

The studies of Refs. 2–4 noted the special significance of $(\omega_A/\omega_\alpha)(V/b\omega_\alpha)$ in terms of the other system parameters and variables. This parameter grouping is a basic system variable and must be matched in order to duplicate system frequency characteristics and system stability characteristics. Therefore, because matching implies that the parameter grouping is a constant, the following equation may be formed:

$$(\omega_A/\omega_\alpha)(V/b\omega_\alpha) = C \tag{5}$$

But, from the definition of ω_A and the Regier number, $R \equiv b\omega_\alpha\mu^{1/2}/a$, this becomes

$$\left[\frac{1}{\mu}\left(\frac{a}{b\omega_\alpha}\right)^2\right] M = \frac{1}{R^2} M = C \tag{6}$$

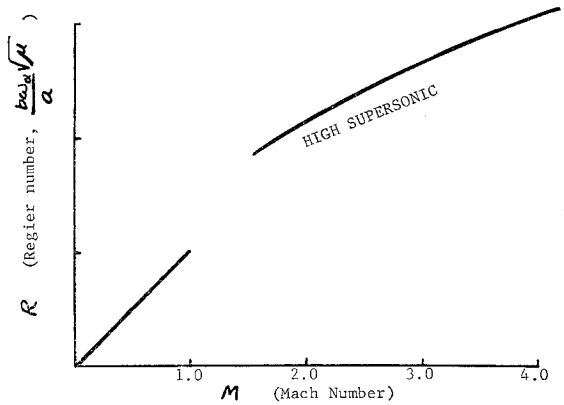

Fig. 1 Regier number vs Mach number.

The normal Regier number plot for subsonic speeds is R vs M, whereas the preceding equation would be more properly plotted as R^2 vs M for a straight line or R vs M for a parabola. Figure 1 illustrates the latter.

The use of a Regier number graph for high supersonic speeds as well as subsonic speeds still leaves the stability characteristics unknown for transonic and supersonic speed. However, examining the parameter grouping more closely, its equivalent in stability derivative form is seen to be

$$\frac{\omega_A}{\omega_\alpha}\frac{V}{b\omega_\alpha} \equiv \frac{C_{L\alpha}\rho V^2}{m\omega_\alpha{}^2} \equiv \left(\frac{C_{L\alpha}\rho a^2}{m\omega_\alpha{}^2}\right) M^2 \tag{7}$$

It is now suggested that μ be redefined as $\mu \equiv m/\rho b^2$; this results in the new expression

$$[(C_{L\alpha}/\mu)(a^2/b^2\omega_\alpha{}^2)]M^2$$

Furthermore, define a new parameter (analogous to Regier number) as $\bar{R}$:

$$\bar{R} \equiv (b\omega_\alpha/a)(\mu/C_{L\alpha})^{1/2} \tag{8}$$

As a result of this definition, $\bar{R}$ vs M may be plotted for all aerodynamic speeds, and this graph, which is a straight line as in Fig. 2, illustrates the torsional stiffness requirements for neutral stability of an aeroelastic surface.

Whether the aeroelastician uses Regier number or its modification presented herein, significant design evaluations may be approximated. One particular conclusion that is used in wind-tunnel flutter-model design may be drawn from the parameter, viz., that flutter speed is in fact independent of mass, since $\mu^{1/2}\omega_\alpha$ is a measure of stiffness and not mass. Also, since $C_{L\alpha}$ varies with Mach number and planform, use of the modified parameter will result in better understanding of flutter characteristics in terms of planform variables.

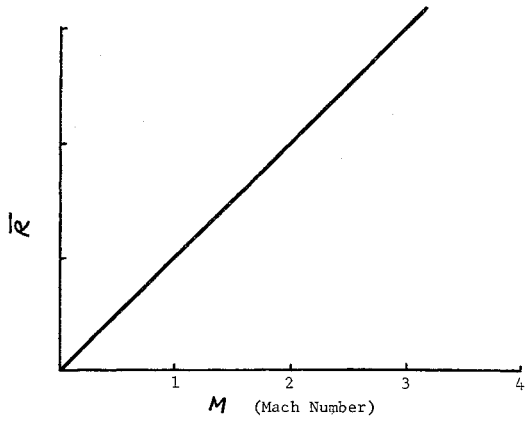

Fig. 2 $\bar{R}$ vs Mach number.

References

[1] Bisplinghoff, R., Ashley, H., and Halfman, R., *Aeroelasticity* (Addison-Wesley Publishing Co., Inc., Cambridge, Mass., 1955), Chap. 3.

[2] Zisfein, M. and Frueh, F., "A study of velocity-frequency-damping relationships for wing and panel binary systems in high supersonic flow," Air Force Office of Scientific Research TN 59-969 (October 1959).

[3] Zisfein, M. and Frueh, F., "Aeroelastic system approximations," Air Force Office of Scientific Research Contractors Solid Mechanics Conference, Pasadena, Calif. (February 1960).

[4] Zisfein, M. and Frueh, F., "Approximation methods for aeroelastic systems in high supersonic flow," Air Force Office of Scientific Research TR 60-182 (October 1960).

Shock-Layer Radiation for Sphere-Cones with Radiative Decay

JIN H. CHIN* AND L. F. HEARNE†
Lockheed Missiles and Space Company, Sunnyvale, Calif.

INTERPLANETARY vehicles re-entering the earth's atmosphere at hyperbolic velocities will be subjected to severe thermal environments. For the extreme re-entry velocities presently being considered in missions analysis, radiation is a major heat-transfer mechanism. Consequently, slender vehicle configurations, such as spherically blunted cones, are attractive.

Manned vehicles may re-enter at velocities in excess of 60,000 fps. Trajectory requirements dictate descent to altitudes of approximately 200,000 ft. At these conditions, the effects of radiative decay in the shock layer become important. Previous investigations of these effects for detached shock layers are reported in Refs. 1–5. The results of these references illustrate the nonadiabatic nature of the shock layer at very high entry velocities. In this note, approximate methods for determination of the effect of radiative decay on the shock-layer radiation toward sphere-cones will be presented. As pointed out in Ref. 5, for most conditions of interest, the effect of self-absorption in the shock layer is small.

As the gas particles travel downstream from the shock wave, the enthalpy decays as a result of radiation loss; that is,

$$-u(dh/ds) = 4k\sigma T^4 \tag{1}$$

where u is the particle velocity, s the distance along the streamline, k the Planck-mean mass absorption coefficient, σ the Stefan-Boltzmann constant, and T the absolute temperature. The change of the particle kinetic energy has been neglected in the energy balance.

For calculation of radiation to the body, the shock layer is approximated by a semi-infinite plane-parallel slab having the local shock-layer thickness and radiation distribution. Then,

$$q = \int_0^{\Delta} 2\rho k\sigma T^4 dy \tag{2}$$

where q is radiation toward body, ρ local density with radiative decay, Δ shock-layer thickness, and y distance from body. Introducing the Howarth-Dorodnitsyn variable $y_a = \int_0(\rho/\rho_s)dy$, Eq. (2) may be written as

$$q = \int_0^{\Delta_a} 2\rho_s k\sigma T^4 dy_a \tag{3}$$

where ρ_s is the density immediately behind shock, and Δ_a is the adiabatic shock-layer thickness. Equation (3) may be transformed to yield

$$\frac{q}{q_a} = \int_0^1 \left(\frac{kT^4}{k_s T_s^4}\right) d\left(\frac{y_a}{\Delta_a}\right) \tag{4}$$

where $q_a \equiv 2\rho_s k_s \sigma T_s^4 \Delta_a$, radiation toward the body from the "adiabatic" shock layer, and where k_s, T_s correspond to conditions immediately behind the shock.

The adiabatic shock-layer thickness may be obtained from the constant-density solutions. For a sphere (Ref. 6, p. 160), this thickness in terms of body radius R is

$$\Delta_a/R = \epsilon/[1 + (\tfrac{8}{3}\epsilon)^{1/2} - \epsilon] \tag{5}$$

where $\epsilon = \rho_\infty/\rho_s$ and ρ_∞ = freestream density. For a cone (Ref. 6, p. 146),

$$\Delta_a/S = \tfrac{1}{2}\epsilon \tan\theta_s \approx \tfrac{1}{2}\epsilon \tan\theta_c \tag{6}$$

where S is the distance from stagnation point along the conical surface, θ_s shock angle, and θ_c cone half-angle.

The particle velocity along the stagnation streamline in the transformed coordinate system is approximated as that given by the incompressible potential flow expression:

$$u = (\rho_\infty u_\infty/\rho)(y_a/\Delta_a) \tag{7}$$

where u_∞ is the freestream velocity. Interpreting $-ds = dy$, Eqs. (1) and (7) may be combined to yield

$$d\ln(y_a/\Delta_a) = (1/\Gamma_s)(k_s T_s^4/kT^4)d(h/h_s) \tag{8}$$

where

$$\Gamma_s \equiv 2q_a/\rho_\infty u_\infty h_s \approx 4q_a/\rho_\infty u_\infty^3$$

and h_s is the enthalpy immediately behind the shock wave.

For the conical body, the local shock layer consists of approximately parallel streamlines that emanate from different positions along the conical shock wave. From a continuity consideration,

$$2\pi(S\sin\theta_c)(u_\infty\cos\theta_s)\rho dy = \pi\rho_\infty u_\infty d[(S - x)\sin\theta_c]^2$$

or, with $\theta_c \approx \theta_s$,

$$\rho dy = -\rho_\infty[1 - (x/S)]\tan\theta_s dx \tag{9}$$

Received March 23, 1964. Portions of the work described in this paper were sponsored by NASA under Contracts NAS 9-1702 and NAS 2-1798. The authors wish to thank D. M. Tellep, Manager, Launch and Entry Thermodynamics, for reviewing the manuscript.

* Staff Engineer, Launch and Entry Thermodynamics, Thermodynamics Division, Flight Technology, Research and Development. Member AIAA.

† Research Specialist, Launch and Entry Thermodynamics, Thermodynamics Division, Flight Technology, Research and Development.